

# Electron Crystal Structure of the Transcription Factor and DNA Repair Complex, Core TFIID

Wei-Hau Chang and Roger D. Kornberg\*

Department of Structural Biology  
Stanford University School of Medicine  
Stanford, California 94305

## Summary

Core TFIID from yeast, made up of five subunits required both for RNA polymerase II transcription and nucleotide excision DNA repair, formed 2D crystals on charged lipid layers. Diffraction from electron micrographs of the crystals in negative stain extended to about 13 Å resolution, and 3D reconstruction revealed several discrete densities whose volumes corresponded well with those of individual TFIID subunits. The structure is based on a ring of three subunits, Tfb1, Tfb2, and Tfb3, to which are appended several functional moieties: Rad3, bridged to Tfb1 by Ssl1; Ssl2, known to interact with Tfb2; and Kin28, known to interact with Tfb3.

## Introduction

TFIID is the largest and most complex of the general transcription factors required for the initiation of transcription by RNA polymerase II (Conaway and Conaway, 1993). It is composed of nine subunits, with a total mass of 0.5 MDa (Table 1). Four subunits impart catalytic activities: two subunits are ATPase/helicases (Sung et al., 1987a, 1987b, 1993; Schaeffer et al., 1993; Guzder et al., 1994a, 1994b), important for melting DNA around the start site of transcription; two subunits form a cyclin-dependent protein kinase (cdk)/cyclin pair (Bootsma and Hoeijmakers, 1993; Schaeffer et al., 1994; Svejstrup et al., 1994), important both for transcriptional regulation and for subsequent RNA processing. All subunits exhibit significant amino acid sequence conservation across species from yeast to humans.

TFIID is also required for nucleotide-excision repair of damaged DNA (Coin and Egly, 1998; de Laat et al., 1999). All subunits except the cdk/cyclin pair form part of an even larger DNA “repairosome” (Svejstrup et al., 1995; Feaver et al., 2000). The dual role of TFIID in transcription and DNA repair has been suggested to underlie the coupling of these two processes (Feaver et al., 1993; Friedberg, 1996). Mutations in the human genes for TFIID subunits are responsible for the DNA repair disease Xeroderma pigmentosum and other congenital disease syndromes (Flejtner et al., 1992; Friedberg, 1992; Schaeffer et al., 1993).

Structural studies of TFIID, essential for understanding its multiple mechanisms, have so far been limited to X-ray analysis of the cdk subunit (Andersen et al., 1997). Such analysis is not readily extended to the entire TFIID or to the related repairosome, due to the large size and low abundance of these complexes. We have

therefore turned to the formation of two-dimensional (2D) crystals on lipid layers and imaging by electron microscopy (Uzgiris and Kornberg, 1983; Ludwig et al., 1986; Ribí et al., 1987; Kornberg and Darst, 1991). This approach has been applied to RNA polymerase II (Edwards et al., 1990; Asturias and Kornberg, 1995; Asturias et al., 1997, 1998), a multiprotein assembly of similar size and complexity to TFIID, revealing the surface topography of the enzyme at about 15 Å resolution (Darst et al., 1991; Jensen et al., 1998). The 2D crystallographic analysis of RNA polymerase II also proved useful for identifying sites of interaction with nucleic acids (Pogliutsch et al., 1999) and general transcription factors (Leuther et al., 1996), and for guiding the production of 3D crystals for X-ray diffraction (Fu et al., 1999).

We report here on the 2D crystallographic analysis of a five-subunit “core” TFIID complex from yeast. This complex results from the loss of the ATPase/helicase Ssl2, the cdk/cyclin pair, and one additional subunit in the course of isolation (Table 1). The complex retains the other ATPase/helicase, Rad3, and also contains Ssl1, Tfb1, Tfb2, and Tfb3 (Feaver et al., 1991; Svejstrup et al., 1994). All five subunits are essential both for transcription and for DNA repair in vivo (Naumovski and Friedberg, 1986; Naumovski and Friedberg, 1987; Guzder et al., 1994a; Matsui et al., 1995; Wang et al., 1995; Sweder et al., 1996; Feaver et al., 1997, 2000). Indeed, functional activity of the core complex has been demonstrated in both transcription and repair assays in vitro (Svejstrup et al., 1994; Sung et al., 1996).

## Results

Core TFIID was purified from yeast with a hexahistidine tag on the Tfb1 subunit as described (Svejstrup et al., 1994), with modifications to improve the homogeneity of the product. Addition of an ammonium sulfate precipitation step, as well as small changes in the elution schedules for chromatography on BioRex and TSK phenyl, gave more complete removal of Ssl2 and the cdk/cyclin pair. The resulting core TFIID preparation contained only the five subunits previously identified and no detectable contaminant (Figure 1).

Core TFIID was crystallized on positively charged lipid layers of the same composition and under similar aqueous solution conditions to those previously employed for RNA polymerase II. The resulting 2D crystals were in the two-sided plane group p1, with unit cell parameters  $a = 82.5 \text{ \AA}$ ,  $b = 119.5 \text{ \AA}$ ,  $\gamma = 116.5^\circ$ . They gave diffraction in negative stain to about 13 Å resolution (Figure 2A), as judged from an average phase residual for 19 images of  $64^\circ$  to this resolution.

For 3D reconstruction of core TFIID, 19 images of untilted crystals and 136 images of crystals tilted up to  $56^\circ$  were used (Figure 3A). The data were 98% complete to an in-plane resolution of 13 Å and  $55^\circ$  tilt angle. A resolution of 18 Å was estimated in the direction perpendicular to the crystal plane ( $z^*$ ) from a point-spread function fitted to the data (Unger and Schertler, 1995). The average phase error of individual measurements along lattice lines within  $0.0025 \text{ \AA}^{-1}$  in  $z^*$  was  $28.5^\circ$ .

\*To whom correspondence should be addressed (e-mail: kornberg@stanford.edu).

Table 1. Yeast TFIIH Subunits and Their Human Homologs

Yeast Subunits	Size (kDa)	Core Subunits	Relative Mass (%)	Human Homolog
Ssl2	95	–		XPB
Rad3	89	+	28.5	XPB
Tfb1	73	+	23.3	p62
Tfb2	59	+	18.9	p55
Ssl1	53	+	16.9	p44
Ccl1	45	–		Cyclin
Tfb3	38	+	12.1	MAT1
Tfb4	37	–		p34
Kin28	35	–		Cdk7

When contoured at  $1\sigma$  above the mean, the 3D structure (Figure 3B) displayed a set of connected densities within a p1 cell that were well separated from the density in adjacent cells (Figure 2B) and therefore appeared to define the molecular boundaries of the TFIIH complex. These boundaries enclosed a volume 68.7% of that expected from the mass of core TFIIH, consistent with the molecular volumes of 3D structures determined in negative stain in the past. The density was clearly divided into three regions, which were provisionally identified with TFIIH subunits, on the basis of the relative volumes of the regions and relative masses of the subunits. The volumes of the three regions were 16.6%, 30.8%, and 52.6% of the total, compared with masses, as fractions of the total for core TFIIH, of 16.9% for Ssl1, 28.5% for Rad3, and 54.3% for a combination of Tfb1, Tfb2, and Tfb3 (Table 1). The regions assigned to Ssl1 and Rad3 appeared roughly ellipsoidal, while that containing the Tfb proteins formed a ring, about 80 Å in outside diameter, with an average thickness of about 30 Å, surrounding a 15 Å hole (lower panel in Figure 3B). A bulge protrudes from the ring toward the junction between Ssl1 and Rad3 (upper panel in Figure 3B).

## Discussion

The arrangement of subunits in core TFIIH suggested here on the basis of the electron crystal structure is generally consistent with biochemical and genetic evidence. A peripheral location of Rad3 in the structure is in keeping with its loss from some preparations of core TFIIH during isolation. Contact of Rad3 with Ssl1 in the structure accords with interaction of these proteins in both two-hybrid studies and coimmunoprecipitation experiments (Bardwell et al., 1994a). A discrepancy arises

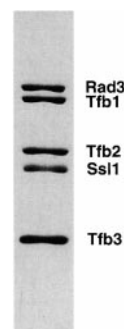


Figure 1. SDS-PAGE of Core TFIIH

A peak fraction (0.6 μg of protein) from Phenyl HPLC, the last step of core TFIIH purification, was resolved in an SDS-10% polyacrylamide gel and revealed by silver staining.

in the case of Rad3 and Tfb3, which are placed in distinct regions of the structure, but which have been shown to interact in a two-hybrid analysis (Feaver et al., 2000). Perhaps an interaction also occurs in the structure following a conformational change, in the context of regulation or the formation of larger transcription and DNA repair complexes.

Ssl1 forms a bridge between Rad3 and Tfb proteins in the structure, and it interacts with both Rad3 and Tfb1 in two-hybrid analyses (Feaver et al., 1993; Bardwell et al., 1994a). The point of contact between Ssl1 and the Tfb ring may identify the location of Tfb1 in the ring (Matsui et al., 1995). Tfb1 is also a point of contact with another general transcription factor, TFIIIE, which recruits TFIIH to the RNA polymerase II transcription initiation complex (Li et al., 1994; Bushnell et al., 1996; Holstege et al., 1996).

Two-hybrid analyses also reveal interactions of Tfb2 with Ssl2, the second ATPase/helicase, and of Tfb3 with Ssl1, Rad3, and Kin28, the protein kinase component of TFIIH (Feaver et al., 1997, 2000). We speculate that Tfb3 corresponds to a bulge of the Tfb ring (upper right part of green density in Figure 3B, upper panel). The Tfb ring evidently plays a central role, separately anchoring four components, the two ATPase/helicases, the protein kinase, and the transcription machinery. Coimmunoprecipitation experiments point to a similar role in DNA repair, with Tfb1 contacting the Rad2 component of the repairosome as well (Bardwell et al., 1994b).

Our ~18 Å resolution electron crystal structure of yeast core TFIIH may be compared with an ~38 Å resolution reconstruction from electron micrographs of single

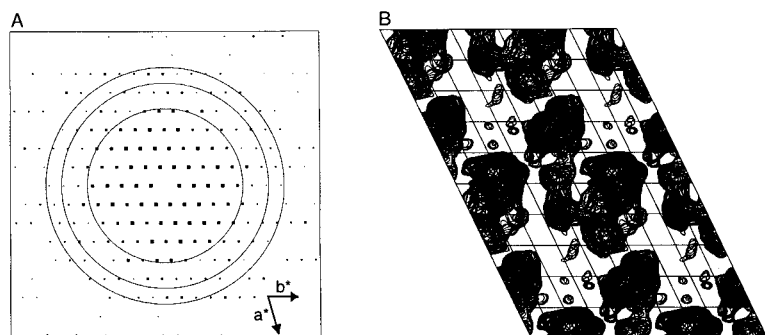


Figure 2. Diffraction from Projected Images of Core TFIIH Crystals and Projected Structure

(A) Combined structure factor data from 19 untilted crystals, displayed as an IQ plot, illustrating data quality and sampling. Larger squares indicate a larger signal-to-noise ratio. Circles indicate 20 Å (innermost), 15 Å, and 13 Å (outermost) resolution.

(B) Projection of the 3D reconstruction in (A) onto the crystal plane, showing the contents of four unit cells, with the density due to one core TFIIH complex in the middle, well resolved from density due to adjacent complexes.

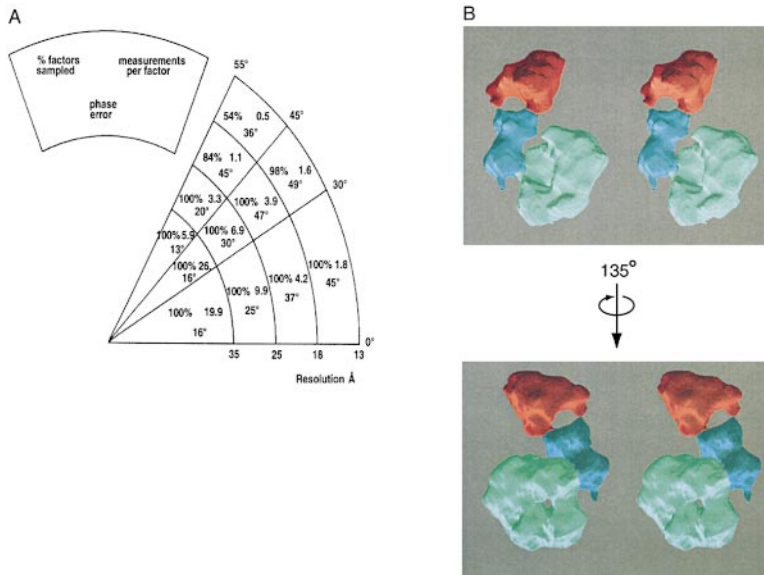


Figure 3. Structure of Core TFIID from 2D Crystals

(A) Reciprocal space coverage in 3D reconstruction of core TFIID. In each region, the number in the upper left is the percentage of possible structure factors that were measured well enough to be sampled. The number in the upper right is the redundancy of measurement, defined as the average number of measurements recorded that lie closer than half the sampling interval  $0.0033 \text{ \AA}^{-1}$  to each structure factor. The number at the bottom is the average phase error, defined as the average phase difference between measurements within  $0.0025 \text{ \AA}^{-1}$  in  $z^*$ .

(B) Stereoviews of the 3D reconstruction of core TFIID at 18 Å resolution, contoured at  $1 \sigma$  above the mean. Colors identify regions of density corresponding in fractional volume with Rad3 (red), Ssl1 (blue), and Tfb1/Tfb2/Tfb3 (green). Upper and lower panels show views related by a clockwise rotation of  $135^\circ$  about a vertical axis in the plans of the figure.

particles of human TFIID (Schultz et al., 2000 [this issue of *Cell*]). The human protein contained all components of the core complex and, in addition, the second ATPase/helicase, homologous to yeast Ssl2, and the protein kinase complex. The approximate locations of the homologs of yeast Rad3, Ssl1, and Kin28 were determined with the use of anti-subunit antibodies. A plausible fit of our crystal structure to the single particle reconstruction could be found (Figure 4), pointing to similarities in size, shape, and arrangement of subunits. According to the fit, the Tfb ring corresponds to a major element of density in the single particle reconstruction (and not to the apparent, much larger ring seen in this reconstruction).

#### Experimental Procedures

##### Core TFIID

*S. cerevisiae* expressing hexahistidine-tagged Tfb1 (Feaver et al., 1993) was grown and fractionated as described (Svejstrup et al., 1994), with the following modifications. Whole cell extract was applied to a BioRex 70 column, washed with buffer A(450) (50 mM HEPES, pH 7.6, with the mM concentration of potassium acetate in parentheses), and eluted with buffer A(750). Elution from the subsequent phosphocellulose column was in a step with buffer A(650), followed by precipitation with ammonium sulfate at 57% of saturation. The precipitate was dissolved in buffer B(0) (50 mM Tris, pH 7.8, with the mM concentration of potassium acetate in parentheses if not stated otherwise), dialyzed against buffer B(300), diluted 3-fold

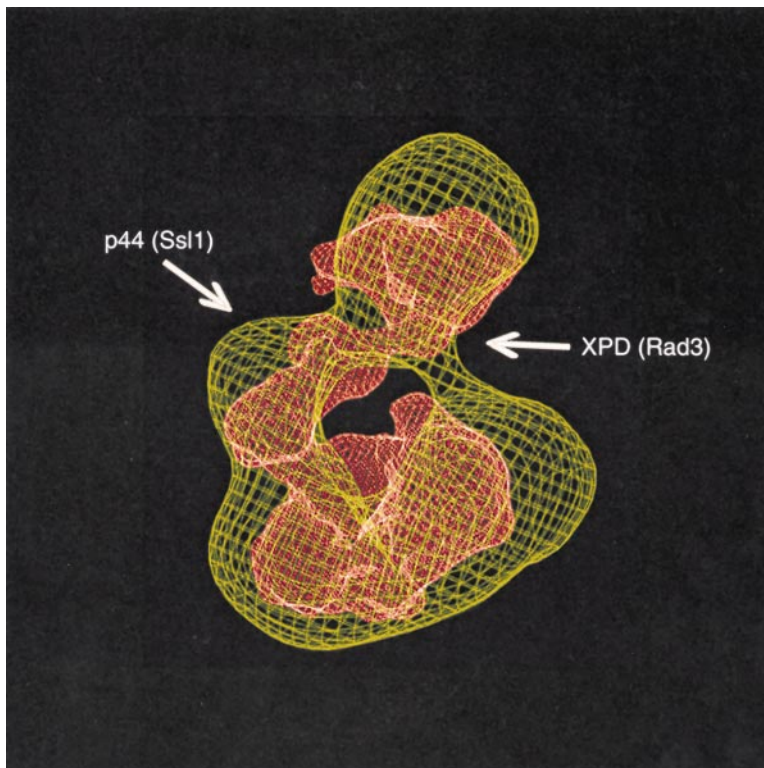


Figure 4. Comparison of Core TFIID Structure from 2D Crystals with HoloTFIID Structure from Single Particle Analysis

The 2D crystal structure of yeast core TFIID reported here (red) is shown superimposed on the single particle structure of human holoTFIID reported by Schultz et al. (2000). Both structures are contoured at a level corresponding to about 60% of the expected volume. Approximate locations of human p44 (yeast Ssl1) and human XPD (yeast Rad3) subunits, as determined by immunolabeling of the human protein, and by assignments of density regions to subunits in the yeast structure, are indicated. The additional volume of the human structure must accommodate the additional subunits present in holoTFIID (Table 1).

with buffer B(0), and applied in batch to 5 ml of Talon metal affinity resin (Clontech) in the presence of 8 mM imidazole for 4 hr. The resin was washed with 50 ml of buffer B(150) containing 8 mM imidazole, and 50 ml of buffer B(400) containing 8 mM imidazole, followed by elution with buffer B(200) containing 100 mM imidazole. Peak fractions of core TFIH were applied to a Mono Q 5/5 column (Pharmacia) equilibrated with buffer B(200). The column was developed with a 20 ml linear gradient from buffer B(400) to B(1400). Peak fractions of core TFIH were adjusted to 500 mM ammonium sulfate and applied to a Phenyl 7.5/7.5 column (TosoHaas) equilibrated with buffer B(500) (50 mM Tris, pH = 7.8, with the mM concentration of ammonium sulfate in parentheses). The column was developed with a 20 ml linear gradient from buffer B(500) to B(70). Core TFIH eluted in an aggregated state between buffer B(200) and B(70). Peak fractions were dialyzed against buffer A(150) containing 10% glycerol, concentrated on a Microcon 100 (Amicon), and stored at  $-80^{\circ}\text{C}$ .

#### Two-Dimensional Crystallization

To a mixture of 10  $\mu\text{l}$  of core TFIH ( $\sim 300$   $\mu\text{g}$  protein/ml) and 20  $\mu\text{l}$  of 50 mM HEPES, pH 7.6, 50  $\mu\text{M}$  ATP, 5mM  $\text{MgCl}_2$ , 5 mM spermidine, 5 mM dithiothreitol in a nylon well (Asturias and Kornberg, 1995) was applied 1  $\mu\text{l}$  of 0.5 mg/ml stearylamine/egg phosphatidylcholine (1:9, w/w) (Avanti Polar Lipids). Following incubation in a humid chamber under argon for 16 hr at  $4^{\circ}\text{C}$ , crystals were harvested by loop-transfer (Asturias and Kornberg, 1995) and applied to a 400-mesh copper/rhodium electron microscope grid (EM Sciences) coated with a continuous carbon film. The grid was blotted with Whatman No. 1 paper, after being washed with 3  $\mu\text{l}$  of 0.05% Tween-20 for 10 s, rinsed with 3  $\mu\text{l}$  of water, stained with 1% uranyl acetate for 40 s, and air-dried.

#### Electron Microscopy and Image Processing

Micrographs were recorded on Kodak SO163 film at a nominal magnification of 35,000 $\times$  or 45,000 $\times$  on a Philips CM12 transmission electron microscope operating at 100 kV in a low dose mode ( $<10$  electrons/ $\text{\AA}^2$ ). Images were obtained from each crystalline area at tilt angles of  $0^{\circ}$ ,  $20^{\circ}$ ,  $35^{\circ}$ ,  $45^{\circ}$ ,  $50^{\circ}$ , and  $55^{\circ}$  at defocus values from about 3000 to 5000  $\text{\AA}$ . Images were checked by optical diffractometry and were digitized at a step size of 10  $\mu\text{m}$  on a Leaf 45 scanner. Structure factors were obtained with the use of an automated suite of MRC programs (Henderson et al., 1986; Jensen et al., 1998; Leuther et al., 1999; Poglitsch et al., 1999), with parameters for lattice indexing and lattice unbending optimized for TFIH crystals. The data set used for 3D reconstruction included 19 untilted crystals, 12 tilted at about  $20^{\circ}$ , 54 at about  $35^{\circ}$ , 35 at about  $45^{\circ}$ , and 35 between  $50^{\circ}$  and  $56^{\circ}$ . Only observations with a signal-to-noise ratio greater than 1.0 (IQ  $> 7$ ) were used. A total of 2632 unique reflections formed a dataset 98% complete to a resolution of 13  $\text{\AA}$  and a maximum tilt angle of  $55^{\circ}$  (Figure 3A).

#### Acknowledgments

We thank our colleagues Francisco Asturias, David Bushnell, Patrick Cramer, Barbara Davis, Jianhua Fu, Avi Gnat, Grant Jensen, Yang Li, and Yuichiro Takagi for technical assistance; John Feaver and Errol Friedberg of Southwestern Medical Center, University of Texas at Dallas, for anti-Rad3 serum; Vinzenz Unger of Yale University, for point-spread-function program and useful discussion on lattice disorder correction. This research was supported by NIH grant AI21144 and by Human Frontiers Science Program grant R.G.-193/97.

Received April 26, 2000; revised June 7, 2000.

#### References

Andersen, G., Busso, D., Poterszman, A., Hwang, J.R., Wurtz, J.M., Ripp, R., Thierry, J.C., Egly, J.M., and Moras, D. (1997). The structure of cyclin H: common mode of kinase activation and specific features. *EMBO J.* 16, 958–967.  
Asturias, F.J., Meredith, G.D., Poglitsch, C.L., and Kornberg, R.D. (1997). Two conformations of RNA polymerase II revealed by electron crystallography. *J. Mol. Biol.* 272, 536–540.  
Asturias, F.J., Chang, W., Li, Y., and Kornberg, R.D. (1998). Electron

crystallography of yeast RNA polymerase II preserved in vitreous ice. *Ultramicroscopy* 70, 133–143.

Asturias, F.J., and Kornberg, R.D. (1995). A novel method for transfer of two-dimensional crystals from the air/water interface to specimen grids. EM sample preparation/lipid-layer crystallization. *J. Struct. Biol.* 114, 60–66.

Bardwell, L., Bardwell, A.J., Feaver, W.J., Svejstrup, J.Q., Kornberg, R.D., and Friedberg, E.C. (1994a). Yeast RAD3 protein binds directly to both SSL2 and SSL1 proteins: implications for the structure and function of transcription/repair factor b. *Proc. Natl. Acad. Sci. USA* 91, 3926–3930.

Bardwell, A.J., Bardwell, L., Iyer, N., Svejstrup, J.Q., Feaver, W.J., Kornberg, R.D., and Friedberg, E.C. (1994b). Yeast nucleotide excision repair proteins Rad2 and Rad4 interact with RNA polymerase II basal transcription factor b (TFIIH). *Mol. Cell. Biol.* 14, 3569–3576.

Bootsma, D., and Hoeijmakers, J.H. (1993). DNA repair. Engagement with transcription. *Nature* 363, 114–115.

Bushnell, D.A., Bamdad, C., and Kornberg, R.D. (1996). A minimal set of RNA polymerase II transcription protein interactions. *J. Biol. Chem.* 271, 20170–20174.

Coin, F., and Egly, J.M. (1998). Ten years of TFIH. *Cold Spring Harb. Symp. Quant. Biol.* 63, 105–110.

Conaway, R.C., and Conaway, J.W. (1993). General initiation factors for RNA polymerase II. *Annu. Rev. Biochem.* 62, 161–190.

Darst, S.A., Edwards, A.M., Kubalek, E.W., and Kornberg, R.D. (1991). Three-dimensional structure of yeast RNA polymerase II at 16  $\text{\AA}$  resolution. *Cell* 66, 121–128.

de Laat, W.L., Jaspers, N.G., and Hoeijmakers, J.H. (1999). Molecular mechanism of nucleotide excision repair. *Genes Dev.* 13, 768–785.

Edwards, A.M., Darst, S.A., Feaver, W.J., Thompson, N.E., Burgess, R.R., and Kornberg, R.D. (1990). Purification and lipid-layer crystallization of yeast RNA polymerase II. *Proc. Natl. Acad. Sci. USA* 87, 2122–2126.

Feaver, W.J., Gileadi, O., and Kornberg, R.D. (1991). Purification and characterization of yeast RNA polymerase II transcription factor b. *J. Biol. Chem.* 266, 19000–19005.

Feaver, W.J., Svejstrup, J.Q., Bardwell, L., Bardwell, A.J., Buratowski, S., Gulyas, K.D., Donahue, T.F., Friedberg, E.C., and Kornberg, R.D. (1993). Dual roles of a multiprotein complex from *S. cerevisiae* in transcription and DNA repair. *Cell* 75, 1379–1387.

Feaver, W.J., Henry, N.L., Wang, Z., Wu, X., Svejstrup, J.Q., Bushnell, D.A., Friedberg, E.C., and Kornberg, R.D. (1997). Genes for Tfb2, Tfb3, and Tfb4 subunits of yeast transcription/repair factor IIF. Homology to human cyclin-dependent kinase activating kinase and IIF subunits. *J. Biol. Chem.* 272, 19319–19327.

Feaver, W.J., Huang, W., Gileadi, O., Myers, L., Gustafsson, C.M., Kornberg, R.D., and Friedberg, E.C. (2000). Subunit interactions in yeast transcription/repair factor TFIH. Requirement for Tfb3 subunit in nucleotide excision repair. *J. Biol. Chem.* 275, 5941–5946.

Fleijter, W.L., McDaniel, L.D., Johns, D., Friedberg, E.C., and Schultz, R.A. (1992). Correction of xeroderma pigmentosum complementation group D mutant cell phenotypes by chromosome and gene transfer: involvement of the human ERCC2 DNA repair gene. *Proc. Natl. Acad. Sci. USA* 89, 261–265.

Friedberg, E.C. (1996). Relationships between DNA repair and transcription. *Annu. Rev. Biochem.* 65, 15–42.

Friedberg, E.C. (1992). Xeroderma pigmentosum, Cockayne's syndrome, helicases, and DNA repair: what's the relationship? *Cell* 71, 887–889.

Fu, J., Gnat, A.L., Bushnell, D.A., Jensen, G.J., Thompson, N.E., Burgess, R.R., David, P.R., and Kornberg, R.D. (1999). Yeast RNA polymerase II at 5  $\text{\AA}$  resolution. *Cell* 98, 799–810.

Guzder, S.N., Qiu, H., Sommers, C.H., Sung, P., Prakash, L., and Prakash, S. (1994a). DNA repair gene RAD3 of *S. cerevisiae* is essential for transcription by RNA polymerase II. *Nature* 367, 91–94.

Guzder, S.N., Sung, P., Bailly, V., Prakash, L., and Prakash, S. (1994b). RAD25 is a DNA helicase required for DNA repair and RNA polymerase II transcription. *Nature* 369, 578–581.

- Henderson, R., Baldwin, J.M., Downing, K.H., Lepault, J., and Zemlin, F. (1986). Structure of purple membrane from *Halobacterium halobium*: record, measurement and evaluation of electron micrographs at 3.5 Å resolution. *Ultramicroscopy* 19, 147–178.
- Holstege, F.C., van der Vliet, P.C., and Timmers, H.T. (1996). Opening of an RNA polymerase II promoter occurs in two distinct steps and requires the basal transcription factors IIE and IIH. *EMBO J.* 15, 1666–1677.
- Jensen, G.J., Meredith, G., Bushnell, D.A., and Kornberg, R.D. (1998). Structure of wild-type yeast RNA polymerase II and location of Rpb4 and Rpb7. *EMBO J.* 17, 2353–2358.
- Kornberg, R.D., and Darst, S.A. (1991). Two-dimensional crystals of proteins on lipid layers. *Curr. Opin. Struct. Biol.* 1, 642–646.
- Leuther, K.K., Bushnell, D.A., and Kornberg, R.D. (1996). Two-dimensional crystallography of TFIIIB- and IIE-RNA polymerase II complexes: implications for start site selection and initiation complex formation. *Cell* 85, 773–779.
- Leuther, K.K., Hammarsten, O., Kornberg, R.D., Chu, G. (1999). Structure of DNA-dependent protein kinase: implications for its regulation by DNA. *EMBO J.* 18, 1114–1123.
- Li, Y., Flanagan, P.M., Tschochner, H., and Kornberg, R.D. (1994). RNA polymerase II initiation factor interactions and transcription start site selection. *Science* 263, 805–807.
- Ludwig, D.S., Ribi, H.O., Schoolnik, G.K., and Kornberg, R.D. (1986). Two-dimensional crystals of cholera toxin B-subunit-receptor complexes: projected structure at 17-Å resolution. *Proc. Natl. Acad. Sci. USA* 83, 8585–8588.
- Matsui, P., DePaulo, J., and Buratowski, S. (1995). An interaction between the Tfb1 and Ssl1 subunits of yeast TFIIH correlates with DNA repair activity. *Nucleic Acids Res.* 23, 767–772.
- Naumovski, L., and Friedberg, E.C. (1986). Analysis of the essential and excision repair functions of the RAD3 gene of *Saccharomyces cerevisiae* by mutagenesis. *Mol. Cell. Biol.* 6, 1218–1227.
- Naumovski, L., and Friedberg, E.C. (1987). The RAD3 gene of *Saccharomyces cerevisiae*: isolation and characterization of a temperature-sensitive mutant in the essential function and of extragenic suppressors of this mutant. *Mol. Gen. Genet.* 209, 458–466.
- Poglitich, C.L., Meredith, G.D., Gnat, A.L., Jensen, G.J., Chang, W.H., Fu, J., and Kornberg, R.D. (1999). Electron crystal structure of an RNA polymerase II transcription elongation complex. *Cell* 98, 791–798.
- Ribi, H.O., Reichard, P., and Kornberg, R.D. (1987). Two-dimensional crystals of enzyme-effector complexes: ribonucleotide reductase at 18-Å resolution. *Biochemistry* 26, 7974–7979.
- Schaeffer, L., Moncollin, V., Roy, R., Staub, A., Mezzina, M., Sarasin, A., Weeda, G., Hoeijmakers, J.H., and Egly, J.M. (1994). The ERCC2/DNA repair protein is associated with the class II BTF2/TFIIH transcription factor. *EMBO J.* 13, 2388–2392.
- Schaeffer, L., Roy, R., Humbert, S., Moncollin, V., Vermeulen, W., Hoeijmakers, J.H., Chambon, P., and Egly, J.M. (1993). DNA repair helicase: a component of BTF2 (TFIIH) basic transcription factor. *Science* 260, 58–63.
- Schultz, P., Fribourg, S., Poterszman, A., Chipoulet, M., Mallouh, V., Moras, D., and Egly, J.M. (2000). Molecular structure of human TFIIH. *Cell* 102, this issue, 599–607.
- Sung, P., Bailly, V., Weber, C., Thompson, L.H., Prakash, L., and Prakash, S. (1993). Human xeroderma pigmentosum group D gene encodes a DNA helicase. *Nature* 365, 852–855.
- Sung, P., Guzder, S.N., Prakash, L., and Prakash, S. (1996). Reconstitution of TFIIH and requirement of its DNA helicase subunits, Rad3 and Rad25, in the incision step of nucleotide excision repair. *J. Biol. Chem.* 271, 10821–10826.
- Sung, P., Prakash, L., Matson, S.W., and Prakash, S. (1987a). RAD3 protein of *Saccharomyces cerevisiae* is a DNA helicase. *Proc. Natl. Acad. Sci. USA* 84, 8951–8955.
- Sung, P., Prakash, L., Weber, S., and Prakash, S. (1987b). The RAD3 gene of *Saccharomyces cerevisiae* encodes a DNA-dependent ATPase. *Proc. Natl. Acad. Sci. USA* 84, 6045–6049.
- Svejstrup, J.Q., Feaver, W.J., LaPointe, J., and Kornberg, R.D. (1994). RNA polymerase transcription factor IIH holoenzyme from yeast. *J. Biol. Chem.* 269, 28044–28048.
- Svejstrup, J.Q., Wang, Z., Feaver, W.J., Wu, X., Bushnell, D.A., Donahue, T.F., Friedberg, E.C., and Kornberg, R.D. (1995). Different forms of TFIIH for transcription and DNA repair: holo-TFIIH and a nucleotide excision repairosome. *Cell* 80, 21–28.
- Sweder, K.S., Chun, R., Mori, T., and Hanawalt, P.C. (1996). DNA repair deficiencies associated with mutations in genes encoding subunits of transcription initiation factor TFIIH in yeast. *Nucleic Acids Res.* 24, 1540–1546.
- Unger, V.M., and Schertler, G.F. (1995). Low resolution structure of bovine rhodopsin determined by electron cryo-microscopy. *Biophys. J.* 68, 1776–1786.
- Uzgiris, E.E., and Kornberg, R.D. (1983). Two-dimensional crystallization technique for imaging macromolecules, with application to antigen–antibody–complement complexes. *Nature* 307, 125–129.
- Wang, Z., Buratowski, S., Svejstrup, J.Q., Feaver, W.J., Wu, X., Kornberg, R.D., Donahue, T.F., and Friedberg, E.C. (1995). The yeast TFB1 and SSL1 genes, which encode subunits of transcription factor IIH, are required for nucleotide excision repair and RNA polymerase II transcription. *Mol. Cell. Biol.* 15, 2288–2293.

